KICS The Korean Institute of Communications and Information Sciences

Available online at www.sciencedirect.com

ScienceDirect

ICT Express 8 (2022) 473–478

www.elsevier.com/locate/icte

Deep learning driven beam selection for orthogonal beamforming with limited feedback

Jinho Choi[a], Moldir Yerzhanova[b], Jihong Park[c], Yun Hee Kim[b,*]

[a] School of Information Technology, Deakin University, Burwood, Australia
[b] Department of Electronics and Information Convergence Engineering, Kyung Hee University, Yongin, Republic of Korea
[c] School of Information and Technology, Deakin University, Geelong, Australia

Received 18 August 2021; received in revised form 1 October 2021; accepted 25 October 2021
Available online 4 November 2021

Abstract

This letter studies deep learning methods for beam selection in multiuser beamforming with limited feedback. We construct a set of orthogonal random beams and allocate the beams to users to maximize the sum rate, based on limited feedback regarding the channel power on the orthogonal beams. We formulate the beam allocation problem as a classification or a regression task using a deep neural network (DNN). The results demonstrate that the DNN-based methods achieve higher sum rates than a conventional limited feedback solution in the low signal-to-noise ratio regime under Rician fading, thanks to their robustness to noisy limited feedback.

Keywords: Downlink beamforming; Deep learning; Limited feedback; Orthogonal beam selection

1. Introduction

Multiuser downlink beamforming has been extensively studied to support multiple users using different beams simultaneously. Solutions for multiuser downlink beamforming have been designed under different scenarios such as signal-to-interference-plus-noise ratio (SINR) balancing problems [1], power minimization problems under SINR constraints [2], and sum rate maximization problems under total power constraints [3]. For such beamforming solutions, an access point (AP) requires not only the channel state information (CSI) from the AP to users, which is referred to as CSI at transmitter (CSIT), but also a time-consuming optimization process.

In general, CSIT can be achieved via channel feedback (from users to the AP), yet is challenged by the limited bandwidth of feedback channels. To resolve this issue, limited feedback is considered in [4] for multiuser beamforming with randomly generated beams. It is shown that randomly generated orthogonal beams with M antennas can provide a full spatial multiplexing gain through a sophisticated user selection with limited feedback for a large number K of users [5,6]. If $M > K$, particularly when $M \gg K$, a different approach has to be considered. In [7], the channel reciprocity was exploited to estimate the CSI from the pilot signals transmitted by users in time division duplexing (TDD). In [8], beam selection was performed for millimeter-wave (mmWave) systems with massive antennas by estimating the received signal-to-noise ratio (SNR) during the beam sweeping step.

By contrast, this paper considers multiuser orthogonal beamforming with limited feedback as in [6] but with a not-so many number of users ($K \leq M$) as in WiFi systems [9]. In particular, we do not assume TDD, warranting the use of limited feedback. In addition, we do not consider a mmWave system offering sharp beams with massive antenna arrays. Instead, our scenario under study is a multiuser multiple input single output (MISO) system equipped with not-so-many antennas, where a different beam should be allocated to each user so as to maximize the sum rate, based on the feedback on the channel power distribution over the orthogonal beams.

With CSIT, the optimal beam allocation can be carried out by solving a combinatorial optimization problem, which may not be desirable due to a high computational complexity for even relatively large M and K. Alternatively, in this work

* Corresponding author.
E-mail addresses: jinho.choi@deakin.edu.au (J. Choi), moldir.yerzhanova@khu.ac.kr (M. Yerzhanova), jihong.park@deakin.edu.au (J. Park), yheekim@khu.ac.kr (Y.H. Kim).

Peer review under responsibility of The Korean Institute of Communications and Information Sciences (KICS).

https://doi.org/10.1016/j.icte.2021.10.008

we aim to solve the multiuser beam allocation problem by leveraging a deep neural network (DNN) that avoids high computing complexity while accommodating limited feedback. The contributions of this paper are summarized as follows.

- We formulate the downlink orthogonal beam allocation as a classification problem, and thereby propose a *DNN classifier* that aims to maximize the sum rate with limited feedback. The DNN input feature vector corresponds to the feedback information on the received power distribution over beams while taking into account measurement noises and quantization errors.
- To reduce the computing complexity of the DNN classifier, we convert the classification problem into a regression task, and propose a *DNN regressor* that is still effective under a low-to-mid SNR regime. This is viable by merging the beam selection combinations into several clusters based on per-user expected sum rates, reducing the DNN output dimension.
- By simulation we show that the proposed DNN frameworks are robust to noisy limited feedback under Rayleigh and Rician fading. Particularly, the proposed methods achieve higher sum rates under Rician fading where the limited feedback is severely distorted by noise and quantization errors.

Related Works. Recently, departing from model-based solutions, model-free approaches leveraging machine learning (ML) and deep learning have been applied to multiantenna system designs. Among plenty of such methods, the following works are notably related to this work, which are broadly categorized into two directions: beamformer fitting and antenna selection. In the first direction, a DNN commonly aims to solve a beamforming problem as a regression task fitting with the solution obtained by a model-based method, such as known optimal multiuser beamforming solutions [2,3,10,11] or suboptimal analog/hybrid beamforming solutions [12,13]. The other direction focuses on an antenna selection problem formulated as a classification task. For single-user multiple input multiple output (MIMO), ML classifiers such as a support vector machine are utilized for antenna selection to minimize the bit error rate [14] or to improve the secrecy rate [15]. For single-user massive MIMO, DNNs are applied for joint antenna selection and digital beamforming so as to optimize the rate [16]. For multiple users, a multi-label DNN is applied for maximizing the sum rate [17].

In both directions, most of studies assume perfect CSIT with known channel matrices [10–13,17], except for single-user scenarios having the element-wise absolute value or power of the perfect channel matrices [14,15] or the channel matrices corrupted by noise [16]. In contrast to these existing works, we consider imperfect CSIT with limited feedback, and study a problem of beam allocation to multiple users for sum rate maximization. We formulate this problem as a classification task, and set the input of the problem (i.e., DNN input feature vector) as the limited feedback information, rather than full CSIT as considered in the existing works. Furthermore, we additionally recast this classification task as a regression task for complexity reduction, which is distinct from the existing regression methods fitting with model-based solutions.

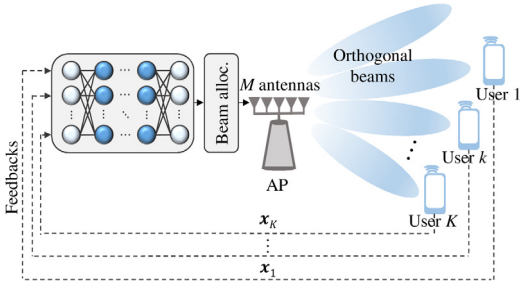

Fig. 1. Multiuser downlink system with orthogonal beam transmission.

Notation: For a vector $\mathbf{x}$, $[\mathbf{x}]_i$ represents the ith element and, for a matrix $\mathbf{X}$, vec($\mathbf{X}$) represents its vectorization. For a set $\mathcal{A}$, $|\mathcal{A}|$ denotes its cardinality. $\mathcal{CN}(\mathbf{a}, \mathbf{R})$ represents the distribution of circularly symmetric complex Gaussian (CSCG) random vectors with mean vector $\mathbf{a}$ and covariance matrix $\mathbf{R}$.

2. System model

Consider a multiuser downlink system where an AP serves K users, as illustrated in Fig. 1. The AP is equipped with M transmit antennas subject to $M \geq K$ and each user is equipped with a single receive antenna. Let $\{\mathbf{w}_m\}_{m=1}^M$ denote M orthonormal beams so that $\mathbf{W} = [\mathbf{w}_1, \mathbf{w}_2, \ldots, \mathbf{w}_M]$ satisfies $\mathbf{W}\mathbf{W}^H = \mathbf{W}^H\mathbf{W} = \mathbf{I}_M$. The orthogonal beam matrix $\mathbf{W}$ is pre-determined and is constructed by any $M \times M$ unitary matrix.

In order to allow users' feedback for beam selection, the AP transmits M orthogonal beams $\{\mathbf{w}_m\}_{m=1}^M$ with the orthonormal pilot sequences $\{\mathbf{s}_m\}_{m=1}^M$ over T ($\geq M$) symbols, where $\mathbf{s}_m = [s_m(1), s_m(2), \ldots, s_m(T)]^{\mathrm{T}}$. The pilot sequence matrix $\mathbf{S} = [\mathbf{s}_1, \mathbf{s}_2, \ldots, \mathbf{s}_M]$ satisfies $\mathbf{S}^H\mathbf{S} = \mathbf{I}_M$. At the kth user, the received signal becomes

$$y_k(l) = \mathbf{h}_k^{\mathrm{H}} \sum_{m=1}^{M} \mathbf{w}_m s_m(l) + n_k(l), \tag{1}$$

where $\mathbf{h}_k^{\mathrm{H}}$ represents the $1 \times M$ channel vector from the AP to user k and $n_k(l) \sim \mathcal{CN}(0, \sigma_k^2)$ is the additive noise with variance σ_k^2. The bank of M correlators can be used to find the composite channel gains, i.e., $\{\mathbf{h}_k^{\mathrm{H}}\mathbf{w}_m\}_{m=1}^M$, at the kth user as follows:

$$z_{k,m} = \sum_{l=1}^{T} y_k(l) s_m^*(l) = \mathbf{h}_k^{\mathrm{H}}\mathbf{w}_m + n_{k,m}, \tag{2}$$

where $n_{k,m} = \sum_{l=1}^{T} n_k(l) s_m^*(l) \sim \mathcal{CN}(0, \sigma_k^2)$. Each user sends the feedback information from $\{z_{k,m}\}_{m=1}^M$ so that the AP can allocate beams to K users, as we shall elaborate in the next section.

3. Beam allocation

This section considers beam allocation at the AP with the feedback information from users.

3.1. Optimal beam allocation

With K users and M antennas, there exist $M_K = \frac{M!}{(M-K)!}$ patterns that allocate a unique beam to each user. For $i = 1, 2, \ldots, M_k$, let $\mathbf{m}_i \in \mathcal{M}$ of length K denote a beam allocation vector, where $|\mathcal{M}| = M_K$ and $[\mathbf{m}_i]_k \in \mathbb{M} = \{1, 2, \ldots, M\}$ represents the beam index of user k. For example, if $M = 3$ and $K = 2$, there are $M_K = 6$ possible allocation patterns: $\mathbf{m}_1 = [1, 2]$, $\mathbf{m}_2 = [1, 3]$, $\mathbf{m}_3 = [2, 1]$, $\mathbf{m}_4 = [2, 3]$, $\mathbf{m}_5 = [3, 1]$, and $\mathbf{m}_6 = [3, 2]$.

With CSIT, i.e., $\mathbf{h}_k$ is known, the AP can compute the signal-to-interference-plus-noise ratio (SINR) at user k for beam allocation $\mathbf{m}$ as follows:

$$\mathsf{SINR}_{k,\mathbf{m}_i} = \frac{|\mathbf{h}_k^{\mathrm{H}} \mathbf{w}_{[\mathbf{m}_i]_k}|^2}{\sum_{l \neq k} |\mathbf{h}_k^{\mathrm{H}} \mathbf{w}_{[\mathbf{m}_i]_l}|^2 + \sigma_k^2}. \tag{3}$$

Under the maximum sum-rate criterion, the optimal beam allocation is given by

$$i^* = \underset{i \in \{1, \ldots, M_K\}}{\operatorname{argmax}} \sum_{k=1}^{K} \log_2 \left(1 + \mathsf{SINR}_{k,\mathbf{m}_i}\right). \tag{4}$$

This requires an exhaustive search of the complexity order $O(M_K)$, which grows exponentially with K. Hereafter, the beam allocation according to (4) is referred to as the *optimal beam allocation*.

3.2. Beam allocation with limited feedback

Without CSIT, $\mathbf{h}_k$ should be reported from user k. To reduce the feedback amount, the user transmits the feature vector

$$\mathbf{x}_k = [|z_{k,1}|^2, |z_{k,2}|^2, \ \ldots \ |z_{k,M}|^2]^{\mathrm{T}}. \tag{5}$$

This only includes M amplitudes, as compared with $\mathbf{h}_k$ that consists of not only M amplitudes but also their phases. The feedback information from K users is available at the AP, which is expressed as $\mathbf{x} = \mathrm{vec}([\mathbf{x}_1, \mathbf{x}_2, \ldots, \mathbf{x}_K])$. This leads to the beam allocation at the AP as follows:

$$i^*(\mathbf{x}) = \underset{i \in \{1, \ldots, M_K\}}{\operatorname{argmax}} \sum_{k=1}^{K} \log_2 \left(1 + \widehat{\mathsf{SINR}}_{k,\mathbf{m}_i}\right), \tag{6}$$

where $\widehat{\mathsf{SINR}}_{k,\mathbf{m}_i}$ is an estimate on the SINR (3) obtained with limited feedback $\mathbf{x}$; In the ideal case, $\widehat{\mathsf{SINR}}_{k,\mathbf{m}_i} = \mathsf{SINR}_{k,\mathbf{m}_i}$ when the background noise in $\mathbf{x}$ vanishes.

To further reduce the feedback amount, each user needs to quantize $\mathbf{x}_k$ with a small number of bits. The AP then receives a quantized version of $\mathbf{x}_k$, i.e., $\hat{\mathbf{x}}_k = Q(\mathbf{x}_k)$, where $Q(\cdot)$ represents a quantization operation. As a result, the AP estimates SINRs from $\hat{\mathbf{x}} = \mathrm{vec}([\hat{\mathbf{x}}_1, \hat{\mathbf{x}}_2, \ldots, \hat{\mathbf{x}}_K])$, and performs the optimal beam allocation with the estimated SINRs. The beam allocation with $\mathbf{x}$ or $\hat{\mathbf{x}}$ is henceforth referred to as the *optimal beam allocation with limited feedback*.

4. Deep learning for beam allocation

This section transforms the beam allocation problem with limited feedback into two standard deep learning tasks.

4.1. Beam allocation as a classification task

We first aim to recast the problem of (6) as a classification task in supervised learning. To this end, each multiuser channel vector $\mathbf{h} = \mathrm{vec}([\mathbf{h}_1, \mathbf{h}_2 \cdots, \mathbf{h}_K])$ is mapped into a pair of unlabeled data $\mathbf{x} \in \mathbb{R}_+^{MK}$ and its ground-truth label $i^*(\mathbf{x}) \in \{1, 2, \ldots, M_K\}$, i.e., $\mathbf{h} \to \{\mathbf{x}, i^*(\mathbf{x})\}$. Consider a deep neural network (DNN) consisting of MK input neurons for $\mathbf{x}$ and M_K output neurons for the one-hot encoded vector $\mathbf{t}$ of i whose ith element is 1 and otherwise 0. The DNN seeks for $i^*(\mathbf{x})$ for a given input $\mathbf{x}$, which coincides with solving (6) as a classification problem.

To be precise, we prepare the DNN training samples by drawing N channel realizations from a given channel distribution. Let $\mathbf{h}_{(n)}$ be the nth realization of the multiuser channel vector set. For each $\mathbf{h}_{(n)} \to \{\mathbf{x}_{(n)}, i^*(\mathbf{x}_{(n)})\}$, the unlabeled input feature vector $\mathbf{x}_{(n)}$ is determined by (5), while the ground-truth label $i^*(\mathbf{x}_{(n)})$ is given by solving (6), e.g., via an exhaustive search. Then, $\{(\mathbf{x}_{(1)}, i^*(\mathbf{x}_{(1)})), \ldots, (\mathbf{x}_{(N)}, i^*(\mathbf{x}_{(N)}))\}$ is used to train the DNN model $\mathcal{D}^C : \mathbf{x} \to i_{\mathbf{v}}(\mathbf{x}) \in \{1, 2, \ldots, M_K\}$ with model weight vector $\mathbf{v}$. The output layer is constructed with the softmax activation, yielding the softmax output $f_{\mathbf{v}}(\mathbf{x})$ that corresponds to an estimate $\hat{\mathbf{t}}(\mathbf{x})$ of the one-hot encoded ground-truth label vector $\mathbf{t}(\mathbf{x})$ of $i^*(\mathbf{x})$.

The final output $i(\mathbf{x})$ of the model is given by the label i that maximizes $[f_{\mathbf{v}}(\mathbf{x})]_i$. The DNN for classification is trained by minimizing the categorical cross-entropy with respect to $\mathbf{v}$:

$$\min_{\mathbf{v}} \ -\sum_{n} \sum_{i=1}^{M_K} [\mathbf{t}(\mathbf{x}_{(n)})]_i \log \left([f_{\mathbf{v}}(\mathbf{x}_{(n)})]_i\right). \tag{7}$$

After training, for a test channel realization $\mathbf{h}'$, by feeding its associated test input feature vector $\mathbf{x}'$, the DNN immediately outputs $i(\mathbf{x}')$ without solving (6).

4.2. Beam allocation as a regression task

While beam allocation as a classification task is effective for small M and K, the number M_K of labels, i.e., DNN output dimension, increases significantly with M and K. For instance, with $M = 8$ and $K = 6$, $M_K = 20{,}160$ that requires a large DNN with a number of training samples.

Alternatively, we aim to reduce the DNN output dimension by transforming the classification problem into a regression task with a novel grouping method. To this end, M_K labels are grouped into MK clusters of which the metrics are represented by the $K \times M$ matrix $\mathcal{C}(\mathbf{x}) = [\mathcal{C}_{k,m}(\mathbf{x})]$. The (k, m)th entry of $\mathcal{C}(\mathbf{x})$ is given by the expected rate of user k using the mth beam over all possible beam patterns as follows:

$$\mathcal{C}_{k,m}(\mathbf{x}) = \frac{1}{|\mathcal{M}_{k,m}|} \sum_{i \in \mathcal{M}_{k,m}} \log_2 \left(1 + \widehat{\mathsf{SINR}}_{k,\mathbf{m}_i}\right), \tag{8}$$

where $\mathcal{M}_{k,m} = \{i \mid [\mathbf{m}_i]_k = m\}$ with $|\mathcal{M}_{k,m}| = M_K/M$. As an example, if $M = 3$ and $K = 2$, we have

$$\begin{aligned} &\mathcal{M}_{1,1} = \{1, 2\}, \ \mathcal{M}_{1,2} = \{3, 4\}, \ \mathcal{M}_{1,3} = \{5, 6\}, \\ &\mathcal{M}_{2,1} = \{3, 5\}, \ \mathcal{M}_{2,2} = \{1, 6\}, \ \mathcal{M}_{2,3} = \{2, 4\}, \end{aligned} \tag{9}$$

where $\mathcal{M}_{1,3} = \{5, 6\}$ since $[\mathbf{m}_5]_1 = [\mathbf{m}_6]_1 = 3$.

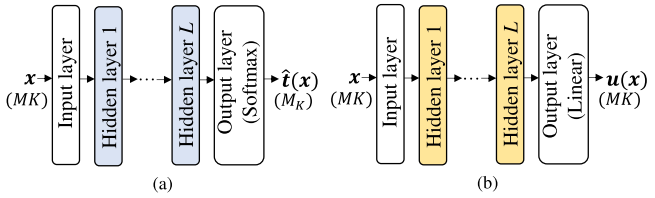

Fig. 2. DNN models: (a) classification (DNN-C) (b) regression (DNN-R).

The regression problem in this paper estimates $\mathcal{C}(\mathbf{x})$ from limited feedback $\mathbf{x}$. Consider a DNN $\mathcal{D}^R : \mathbf{x} \to \mathbf{u}_{\mathbf{v}}(\mathbf{x}) \in \mathbb{R}^{MK}$ with model weight vector $\mathbf{v}$. The input $\mathbf{x}$ is a realization of the limited feedback and the output is $\mathbf{u}_{\mathbf{v}}(\mathbf{x}) = \text{vec}(\mathbf{U}_{\mathbf{v}}(\mathbf{x}))$, where $\mathbf{U}_{\mathbf{v}}(\mathbf{x}) = [u_{k,m;\mathbf{v}}(\mathbf{x})]$ is an estimate on $\mathcal{C}(\mathbf{x})$. Then, the DNN for regression is trained by minimizing the mean square error (MSE) between $\text{vec}(\mathcal{C}(\mathbf{x}))$ and its estimate $\mathbf{u}_{\mathbf{v}}(\mathbf{x})$ with respect to the DNN weight $\mathbf{v}$:

$$\min_{\mathbf{v}} \sum_{n} ||\text{vec}(\mathcal{C}(\mathbf{x}_{(n)})) - \mathbf{u}_{\mathbf{v}}(\mathbf{x}_{(n)})||^2. \tag{10}$$

After training, we perform a test process which leads to the DNN output $\mathbf{u}_{\mathbf{v}^*}(\mathbf{x}')$ for a channel realization $\mathbf{h}'$ and its associated feature vector $\mathbf{x}'$ used in the test. With $\mathbf{U}_{\mathbf{v}^*}(\mathbf{x}') = [u_{k,m;\mathbf{v}^*}(\mathbf{x}')]$, a unique beam is allocated to each user in a way of increasing the sum rate, i.e., increasing the expected rate $u_{k,m;\mathbf{v}^*}(\mathbf{x}')$ of user k by using the mth beam. For this purpose, we select K user-beam pairs $\{(k_j, m_j), j \in \mathbb{K} \triangleq \{1, 2, \ldots, K\}\}$ by sequentially finding the pair having the largest value in $\mathbf{U}_{\mathbf{v}^*}(\mathbf{x}')$ after removing the selected beams and users previously, i.e.,

$$(k_j^*, m_j^*) = \underset{k \in \mathbb{K}\setminus\{k_1^*,\ldots,k_{j-1}^*\},\, m \in \mathbb{M}\setminus\{m_1^*,\ldots,m_{j-1}^*\}}{\arg\max} u_{k,m;\mathbf{v}^*}(\mathbf{x}'), \text{ for } j \in \mathbb{K}. \tag{11}$$

Hereafter, the DNNs solving (7) and (10) are referred to as DNN-C and DNN-R, respectively. To solve these problems, we consider the DNN models with the multilayer perceptron (MLP) architecture comprising L hidden layers and the Rectified Linear Unit (ReLU) activation. For $X \in \{C, R\}$, the model configuration of DNN-X is described as $\mathcal{D}^X(\mathcal{I}, \alpha_1, \ldots, \alpha_L, \mathcal{O})$, where $\mathcal{I}$ and $\mathcal{O}$ denote the input and output dimensions, respectively, and α_l is the number of neurons at the lth hidden layer. The structures of DNN-C and DNN-R are illustrated in Fig. 2.

5. Performance evaluation

We evaluate the performance of the proposed DNN-based beam allocation with limited feedback in Rayleigh and Rician fading channels. The channel samples for Rayleigh fading are generated from iid complex Gaussian vectors as $\mathbf{h}_k \sim \mathcal{CN}(\mathbf{0}, \mathbf{I}_M)$ whilst those for Rician fading are generated by adopting the Saleh–Valenzuela channel model with one line-of-sight (LoS) component and 4 non-LoS components [12].

We obtain appropriate DNN configurations by using the training, validation, and test data sets consisting of 128k, 32k, 40k samples, respectively, unless otherwise stated. The

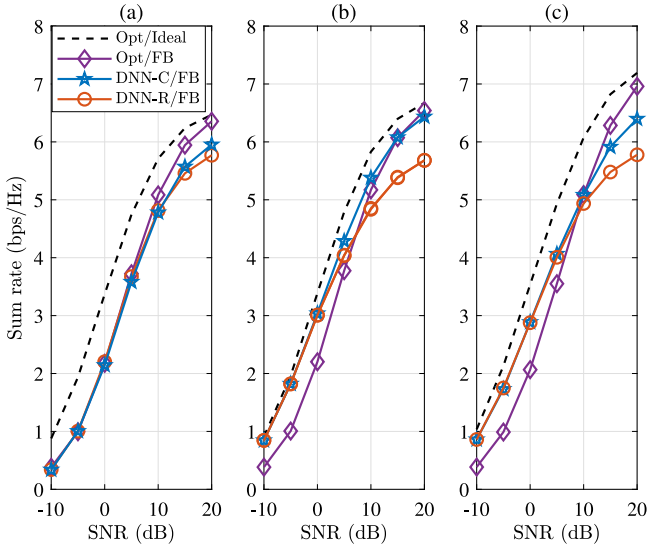

Fig. 3. Average sum rate of beam allocation methods with unquantized feedback; (a) $(M, K) = (8, 3)$ in Rayleigh fading (b) $(M, K) = (8, 3)$ in Rician fading (c) $(M, K) = (16, 3)$ in Rician fading.

DNNs are trained using Python 3.7.10, TensorFlow 2.4.1, and Keras 2.4.0. The DNN model used for each (M, K) setup is trained by using the Adam optimizer with the learning rate 10^{-3} until the validation loss remains unchanged for 10 consecutive epochs. We obtain $\mathcal{D}^C(24, 48, 64, 128, 256, 336)$ and $\mathcal{D}^R(24, 196, 120, 72, 48, 24)$ for $(M, K) = (8, 3)$ and $\mathcal{D}^C(48, 256, 512, 1024, 2048, 3360)$ and $\mathcal{D}^R(48, 480, 240, 120, 80, 48)$ for $(M, K) = (16, 3)$, with $L = 4$.

Fig. 3 provides the average sum rate of the system with unquantized feedback $\mathbf{x}$. The performance is evaluated with $(M, K) = (8, 3)$ and Rayleigh fading in Fig. 3(a), $(M, K) = (8, 3)$ and Rician fading with Rician factor $\kappa_o = 2$ in Fig. 3(b), and $(M, K) = (16, 3)$ and Rician fading with Rician factor $\kappa_o = 2$ in Fig. 3(c). Here, DNN-C/FB and DNN-R/FB represent the DNN methods and Opt/FB represents the exhaustive search in (4). Opt/Ideal is added to serve as an upper bound on the performance of the system that can be achieved with $\mathbf{x}$ having no noise. With the noisy feedback, the performance of DNN-C/FB and DNN-R/FB is close to or even superior to that of Opt/FB in the low SNR region. The gain of the DNN methods over the optimal search in Rician fading is due to the LoS component common to training and data helps to reduce the ambiguity of the noisy feedback during the training process via time-averaging.

In the high SNR region, DNN-C/FB suffers from a loss compared with Opt/FB that is larger in Rayleigh fading or with a larger M due to the curse of dimensionality. The loss can be reduced by increasing the number of training samples but at the cost of complexity. DNN-R induces an additional loss due to its inherent suboptimality. Nonetheless, in return it reduces the model complexity and training time as we will discuss later.

Figs. 4(a) and 4(b) illustrate the impact of the quantized feedback $\hat{\mathbf{x}}$ on the average sum rate under the channel and system conditions of Figs. 4(a) and 4(b), respectively. The

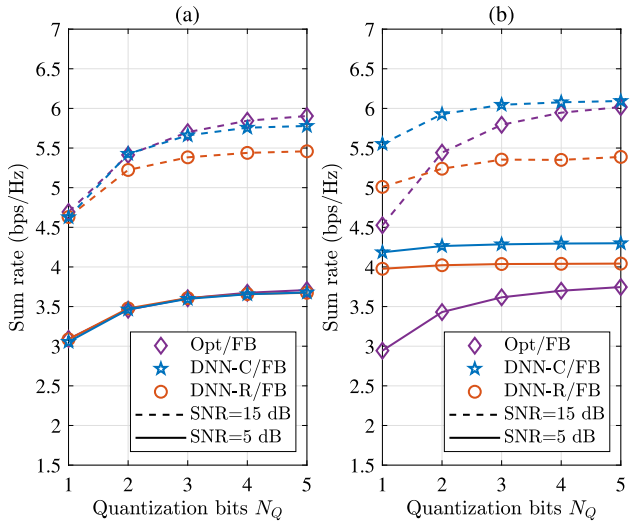

Fig. 4. Average sum rate of beam allocation methods with quantized feedback as the number N_Q of quantization bits increases; (a) $(M, K) = (8, 3)$ in Rayleigh fading (b) $(M, K) = (8, 3)$ in Rician fading.

number of training samples is increased by five times for Rayleigh fading in Fig. 4(a). We adopt a companded quantization $Q(x)$ with 2^{N_Q} levels for the feedback by using the cumulative distribution function $F(x)$ of $x_{k,m}$ for Rayleigh fading by assuming that the AP and users are ignorant of the exact channel distribution. The smaller the number N_Q of quantization bits becomes, the more the performance is degraded for all methods. The degradation is less prominent at a lower SNR value since the noise in $x_{k,m}$, rather than the quantization error, dominates the performance. In Rayleigh fading, the DNN methods cannot provide a better performance than the optimal beam selection as observed in Fig. 4(a). However, the DNN methods outperform the optimal beam selection with quantized feedback in Rician fading since they can extract the common information in the noisy feedback during the training process.

Finally, we report the computation time of the DNN methods and a conventional exhaustive search method on the server with Intel Xeon CPU@2.2 GHz and NVIDIA GPU Tesla T4 in Table 1. DNN-C/FB and DNN-R/FB train 160k data for 30 epochs, and then predict the solutions of 40k test data, while Opt/FB finds the solutions of 40k test data using Python. Due to the larger output dimension and model parameters, DNN-C/FB takes longer training time than DNN-R/FB. Nonetheless, owing to the parallel GPU processing power, the training time increase is not so large as compared with the model parameter increase. The results show that DNN-R can reduce the training time of DNN-C by half when $(M, K) = (16, 3)$. Thus, DNN-R is preferable in a low SNR regime, wherein it achieves a sum rate with lower computing time compared to DNN-C. Next, after training completes, DNN methods provide the solutions by up to 260x and 2600x faster than the optimal search under $(M, K) = (8, 3)$ and $(16, 3)$, respectively. Furthermore, the training cost of DNN methods becomes negligible when $(M, K) = (16, 3)$, under which the integrated training and prediction time of DNN methods is still 5.9x shorter than the prediction time of the optimal search.

Table 1
Computation time of DNN and conventional methods.

(M, K)	Methods	Model parameters	Training time	Prediction time
(8,3)	DNN-C/FB	132,032	415 s	1.35 s
	DNN-R/FB	41,932	375 s	1.35 s
	Opt/FB	–	–	352 s
(16,3)	DNN-C/FB	9,653,280	752 s	1.74 s
	DNN-R/FB	181,448	359 s	1.35 s
	Opt/FB	–	–	3540 s

6. Conclusions

We studied orthogonal beam allocation with limited feedback for a downlink multiuser system where an AP supports each user with one beam. We showed that the problem can be solved by the DNN in classification (DNN-C) and regression (DNN-R). In general, DNN-C provided the performance close to the optimal search while DNN-R provided a suboptimal performance at a reduced complexity. Although DNN-based methods exhibited some loss in the high SNR region of Rayleigh fading, they outperformed the optimal one with noisy feedback in Rician fading, where the LoS component helps to reduce the noise and quantization error through time-domain averaging during the training process.

CRediT authorship contribution statement

Jinho Choi: Conceptualization, Methodology, Writing. **Moldir Yerzhanova:** Software, Investigation. **Jihong Park:** Methodology, Writing. **Yun Hee Kim:** Methodology, Supervision, Writing.

Declaration of competing interest

The authors declare that they have no known competing financial interests or personal relationships that could have appeared to influence the work reported in this paper.

Acknowledgments

This research was supported by the Australian Government through the Australian Research Council's Discovery Projects funding scheme (DP200100391) and by the Ministry of Science and ICT, Korea, through the National Research Foundation of Korea (NRF) (NRF-2021R1A2C1005869) and the Institute for Information & Communications Technology Planning & Evaluation (IITP) under Information Technology Research Center (ITRC) support program (IITP-2021-0-02046).

References

[1] M. Schubert, H. Boche, Solution of the multiuser downlink beamforming problem with individual SINR constraints, IEEE Trans. Veh. Technol. 53 (1) (2004) 18–28.

[2] A. Wiesel, Y.C. Eldar, S. Shamai, Linear precoding via conic optimization for fixed MIMO receivers, IEEE Trans. Signal Process. 54 (1) (2006) 161–176.

[3] S.S. Christensen, R. Agarwal, E. De Carvalho, J.M. Cioffi, Weighted sum-rate maximization using weighted MMSE for MIMO-BC beamforming design, IEEE Trans. Wirel. Commun. 7 (12) (2008) 4792–4799.

[4] M. Sharif, B. Hassibi, On the capacity of MIMO broadcast channels with partial side information, IEEE Trans. Inform. Theory 51 (2) (2005) 506–522.

[5] T. Yoo, N. Jindal, A. Goldsmith, Multi-antenna downlink channels with limited feedback and user selection, IEEE J. Sel. Areas Commun. 25 (7) (2007) 1478–1491.

[6] K. Huang, J.G. Andrews, R.W. Heath Jr., Performance of orthogonal beamforming for SDMA with limited feedback, IEEE Trans. Veh. Technol. 58 (1) (2009) 152–164.

[7] T.L. Marzetta, Noncooperative cellular wireless with unlimited numbers of base station antennas, IEEE Trans. Wirel. Commun. 9 (11) (2010) 3590–3600.

[8] P. Wang, Y. Li, L. Song, B. Vucetic, Multi-gigabit millimeter wave wireless communications for 5G: from fixed access to cellular networks, IEEE Commun. Mag. 53 (1) (2015) 168–178.

[9] E. Perahia, M.X. Gong, Gigabit wireless LANs: An overview of IEEE 802.11ac and 802.11ad, ACM SIGMOBILE Mob. Comput. Commun. Rev. 15 (3) (2011) 23–33.

[10] H. Huang, Y. Song, J. Yang, W. Xia, G. Gui, Fast beamforming design via deep learning, IEEE Trans. Veh. Technol. 69 (1) (2020) 1065–1069.

[11] W. Xia, G. Zheng, Y. Zhu, J. Zhang, J. Wang, A.P. Petropulu, A deep learning framework for optimization of MISO downlink beamforming, IEEE Trans. Commun. 68 (3) (2020) 1866–1880.

[12] H. Huang, Y. Song, J. Yang, G. Gui, F. Adachi, Deep-learning-based millimeter-wave massive MIMO for hybrid precoding, IEEE Trans. Veh. Technol. 68 (3) (2019) 3027–3032.

[13] M.A. Almagboul, F. Shu, A.M.S. Abdelgader, Deep-learning based phase-only robust massive MU-MIMO hybrid beamforming, IEEE Commun. Lett. 25 (7) (2021) 2280–2284.

[14] J. Joung, Machine learning-based antenna selection in wireless communications, IEEE Commun. Lett. 20 (11) (2016) 2241–2244.

[15] D. He, C. Liu, T.Q.S. Quek, H. Wang, Transmit antenna selection in MIMO wiretap channels: A machine learning approach, IEEE Wirel. Commun. Lett. 7 (4) (2018) 634–637.

[16] A.M. Elbir, K.V. Mishra, Joint antenna selection and hybrid beamformer design using unquantized and quantized deep learning networks, IEEE Trans. Wirel. Commun. 19 (3) (2020) 1677–1688.

[17] W. Yu, T. Wang, S. Wang, Multi-label learning based antenna selection in massive MIMO systems, IEEE Trans. Veh. Technol. 70 (7) (2021) 7255–7260.